

DOI: 10.1002/adsc.200800779

# Recyclable Polymer- and Silica-Supported Ruthenium(II)-Salen Bis-pyridine Catalysts for the Asymmetric Cyclopropanation of Olefins

Christopher S. Gill,<sup>a</sup> Krishnan Venkatasubbaiah,<sup>a</sup> and Christopher W. Jones<sup>a,b,\*</sup><sup>a</sup> School of Chemical & Biomolecular Engineering, Georgia Institute of Technology, 311 Ferst Drive NW, Atlanta, Georgia 30332, USA

Fax: (+1)-404-894-2866; phone: (+1)-404-385-1683; e-mail: cjones@chbe.gatech.edu

<sup>b</sup> School of Chemistry and Biochemistry, Georgia Institute of Technology, 901 Atlantic Dr., Atlanta, Georgia 30332, USA

Received: December 16, 2008; Revised: April 8, 2009; Published online: June 3, 2009

Supporting information for this article is available on the WWW under <http://dx.doi.org/10.1002/adsc.200800779>.

**Abstract:** Homogeneous ruthenium(II)-salen bis-pyridine complexes are known to be highly active and selective catalysts for the asymmetric cyclopropanation of terminal olefins. Here, new methods of heterogenization of these Ru-salen catalysts on polymer and porous silica supports are demonstrated for the facile recovery and recycle of these expensive catalysts. Activities, selectivities, and recyclabilities are investigated and compared to the analogous homogeneous and other supported catalysts for asymmetric cyclopropanation reactions. The catalysts are characterized with a variety of methods including solid state cross-polarization magic-angle spinning (CP MAS) <sup>13</sup>C and <sup>29</sup>Si NMR, FT-IR, elemental analysis, and thermogravimetric analysis. Initial investigations produced catalysts possessing high selectivities but decreasing activities upon reuse. Addition of excess pyridine during the washing steps between

cycles was observed to maintain high catalytic activities over multiple cycles with no impact on selectivity. Polymer-supported catalysts showed superior activity and selectivity compared to the porous silica-supported catalyst. Additionally, a longer, flexible linker between the Ru-salen catalyst and support was observed to increase enantioselectivity and diastereoselectivity, but had no effect on activity of the resin catalysts. Furthermore, the polymer-supported Ru-salen-Py<sub>2</sub> catalysts were found to generate superior selectivities and yields compared to other leading heterogeneous asymmetric cyclopropanation catalysts.

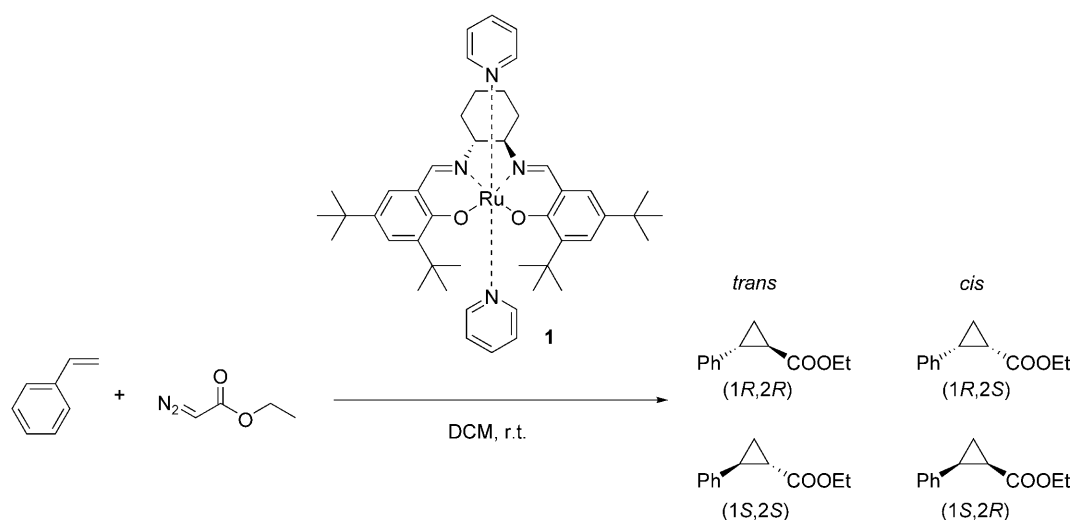
**Keywords:** asymmetric cyclopropanation; enantioselectivity; heterogeneous catalysis; ruthenium-salen; supported catalysts

## Introduction

Asymmetric synthesis of chiral cyclopropyl chemicals is of particular importance in the pharmaceutical and agro-chemical industries as an alternative method of procuring these important chiral building blocks used in the preparation of drugs and pesticides.<sup>[1]</sup> Researchers have developed numerous homogeneous catalysts to facilitate synthesis of these chiral cyclopropyl products.<sup>[2]</sup> Optimizing catalysts to produce desired products in high atom economy has been of particular importance. Consequently, all asymmetric cyclopropanation catalysts are judged based on their activity, diastereoselectivity to *cis* or *trans* cyclopropyl products, and enantioselectivities (*ee*) of the resulting *cis* and *trans* products. Recently, ruthenium-salen catalysts

have been shown to demonstrate high activities and selectivities for the cyclopropanation of olefins (Scheme 1), while maintaining functional group tolerance for a range of electronically diverse olefins.<sup>[3,4]</sup>

With advancements in homogeneous asymmetric cyclopropanation catalysis, several researchers have been working on the development of supported, single-sited heterogeneous catalysts in parallel. Immobilization of these catalysts on solid phase supports allows for the facile recovery and reuse of the asymmetric catalyst, which can be important for a variety of economic, environmental, and quality control reasons. Research in this area has mainly focused on supported copper, rhodium, and ruthenium complexes.<sup>[5,6]</sup> While much research has focused on supported copper bis(oxazoline) (Box) and related complexes,<sup>[6]</sup>



**Scheme 1.** Ru(II)-salen bis-pyridine-catalyzed asymmetric cyclopropanation of styrene with ethyl diazoacetate.

increasing reports of supported ruthenium catalysts have appeared due to their high activity, selectivity, and the advantages of ruthenium over the copper-based systems: superior diastereoselectivities, functional group tolerance, and ease of use. These reports include ruthenium pyridine-bis(oxazoline) (PyBox) complexes grafted to polymers,<sup>[7,8]</sup> encapsulated within polymers,<sup>[9]</sup> and grafted to silica.<sup>[10]</sup> Additional examples of polymer-<sup>[11]</sup> and silica-supported<sup>[12]</sup> ruthenium porphyrins exist. Despite the promising results of homogeneous Ru-salen cyclopropanation catalysts, no reports of Ru-salen catalysts covalently grafted to solid supports exist at present. Only a single report of Ru-salen catalysts coordinated to poly(4-vinylpyridine) for aldehyde olefination has appeared, but this catalyst was hampered by poor recyclability due to leaching of the active Ru-salen catalyst by dissociation of the Ru–N coordination to the polymer support,<sup>[13]</sup> thus highlighting the need for covalent immobilization to solid supports.

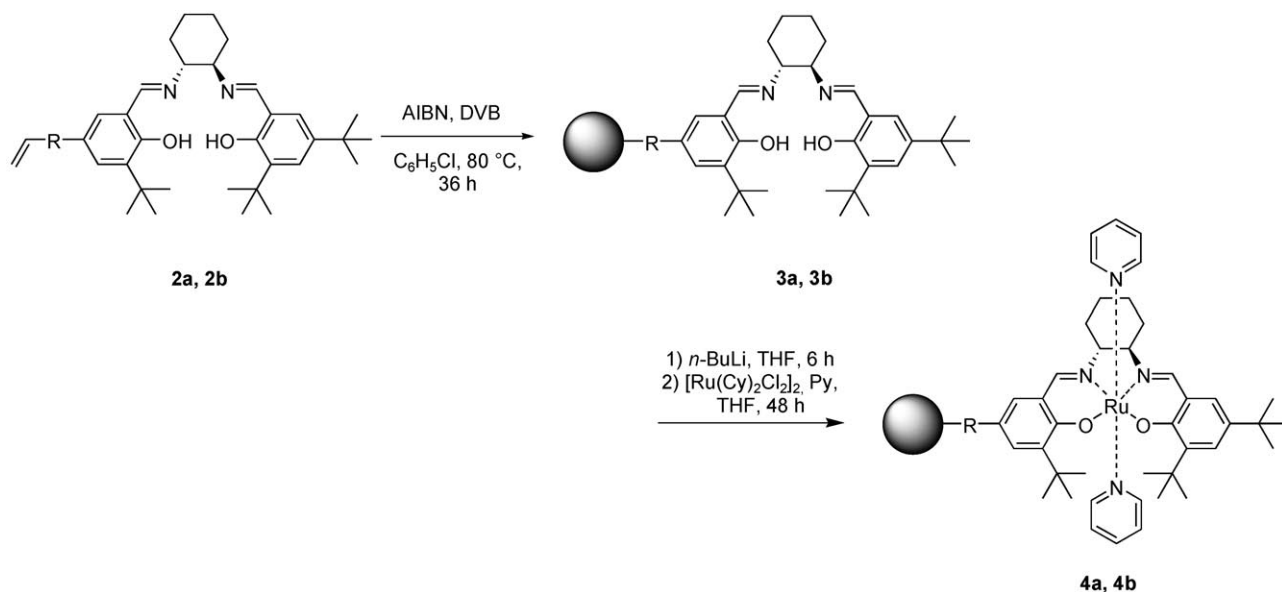
Building on past work in our research group focused on development of supported Co-salen catalysts,<sup>[14–17]</sup> alternative techniques are developed here to provide the first report of heterogenized Ru-salen complexes covalently grafted to solid supports. The goal of this work was to develop a solid catalyst, stable over multiple cycles, that retained the high activity, diastereoselectivity, and enantioselectivities exhibited by the homogeneous analogue in the asymmetric cyclopropanation of olefins with ethyl diazoacetate (EDA). This was accomplished *via* the immobilization of monofunctionalized, unsymmetrical, chiral salen ligands on polymer and silica supports to eventually produce covalently bound, surface-grafted Ru(II)-salen bis-pyridine catalysts. These catalysts were characterized *via* solid state CP MAS <sup>13</sup>C and <sup>29</sup>Si NMR, FT-IR, elemental analysis, and thermogra-

vimetric analysis. This report highlights the synthesis and characterization of these immobilized catalysts, as well as investigations into their activity, selectivity, and recyclability in the cyclopropanation of styrene and other terminal olefins. Additionally, these polymer supported Ru-salen-Py<sub>2</sub> catalysts generated superior yields and selectivities compared to other leading solid-supported asymmetric cyclopropanation catalysts.

## Results and Discussion

### Ruthenium(II)-Salen Bis-Pyridine Polymer Resin Catalysts (4a, 4b): Synthesis and Characterization

Borrowing from previous work developed in our research group, styrene-modified mono-functionalized, unsymmetrical, chiral salen monomers (**2a**, **2b**) were synthesized.<sup>[15,17–19]</sup> These styrene-modified salen compounds were utilized in the synthesis of polymer- and silica-supported materials. Mono-functionalized, unsymmetrical salen ligands were preferred (in comparison to bi-functionalized, symmetric, bis-styryl modified salen ligands<sup>[20]</sup>) due to the greater degree of flexibility and increased distance from the polymer support imparted on the pendant catalyst site. In the proposed bimetallic transition state of the Co-salen-catalyzed hydrolytic kinetic resolution (HKR) mechanism, this flexibility greatly affected the catalyst performance.<sup>[14,21]</sup> In the monometallic mechanism of the Ru-salen cyclopropanation reaction, this flexibility could be less important. However, the linker does impact the steric hindrance of the polymer backbone near the catalytically active site, which can be important for polymer-supported catalysts in general. Insoluble, cross-linked, salen-functionalized polymer



**Scheme 2.** Synthesis of polymer resin-supported Ru(II)-salen bis-pyridine catalysts [**a**: R =  $-\text{C}_6\text{H}_4-$ , **b**: R =  $-\text{C}_6\text{H}_4-\text{CH}_2-\text{O}-(\text{CH}_2)_2-\text{O}-\text{CH}_2-$ ].

resins (**3a**, **3b**) were synthesized in high yield by reaction of the styryl-salen monomers with divinylbenzene (Scheme 2). Ruthenium(II)-salen bis-pyridine polymer resin catalysts (**4a**, **4b**) were then synthesized following modified published procedures<sup>[3]</sup> by initial treatment with *n*-butyllithium to deprotonate the phenolic protons of the salen ligand, followed by metallation with dichloro(*p*-cymene)ruthenium(II) dimer in the presence of excess pyridine. Elemental analysis indicated a ruthenium loading of 0.34 mmol/g at a 6.2:1 N:Ru ratio and 48% metallation efficiency for **4a**, and 0.37 mmol/g ruthenium at a 5.7:1 N:Ru ratio and 53.5% metallation efficiency for **4b**. Moderate metallation efficiencies are common when working with solid supports and likely resulted from reacting stoichiometric equivalents of *n*-butyllithium (2:1) and ruthenium dimer (0.5:1) to the solid-supported salen. This metallation procedure was sufficient for small molecule Ru-salen complexes,<sup>[3]</sup> but was likely hindered by transport issues with the support. Extended reaction times at ambient temperature were utilized to maximize the metallation efficiency.

The successful formation of the Ru(II)-salen-Py<sub>2</sub> complex was evidenced by FT-IR analysis (Figure 1). The characteristic imine stretch appeared at 1628 cm<sup>-1</sup> for **3b**. Upon complexation with ruthenium, there was a sharp decrease in intensity of this band as it shifted towards lower frequencies at 1600 cm<sup>-1</sup>, resulting from a shift of electron density from the imine towards ruthenium.<sup>[22]</sup> Additional support for the formation of the Ru-salen complex was seen in the shift of the carbon-oxygen stretch of the phenolic oxygen. The non-metallated complex displayed a moderate peak at 1270 cm<sup>-1</sup>, characteristic of the ν<sub>C-O</sub> stretch.<sup>[23]</sup>

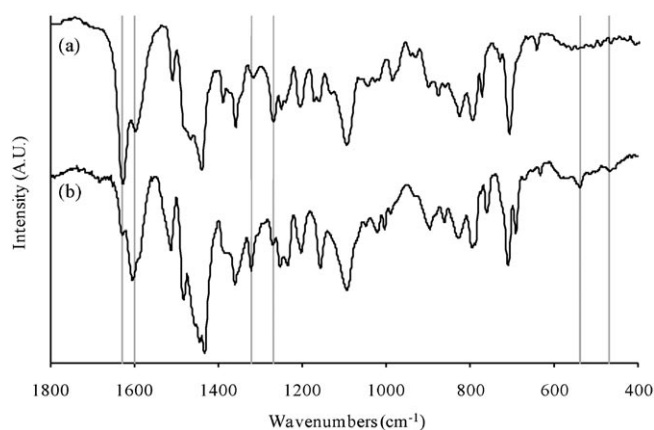
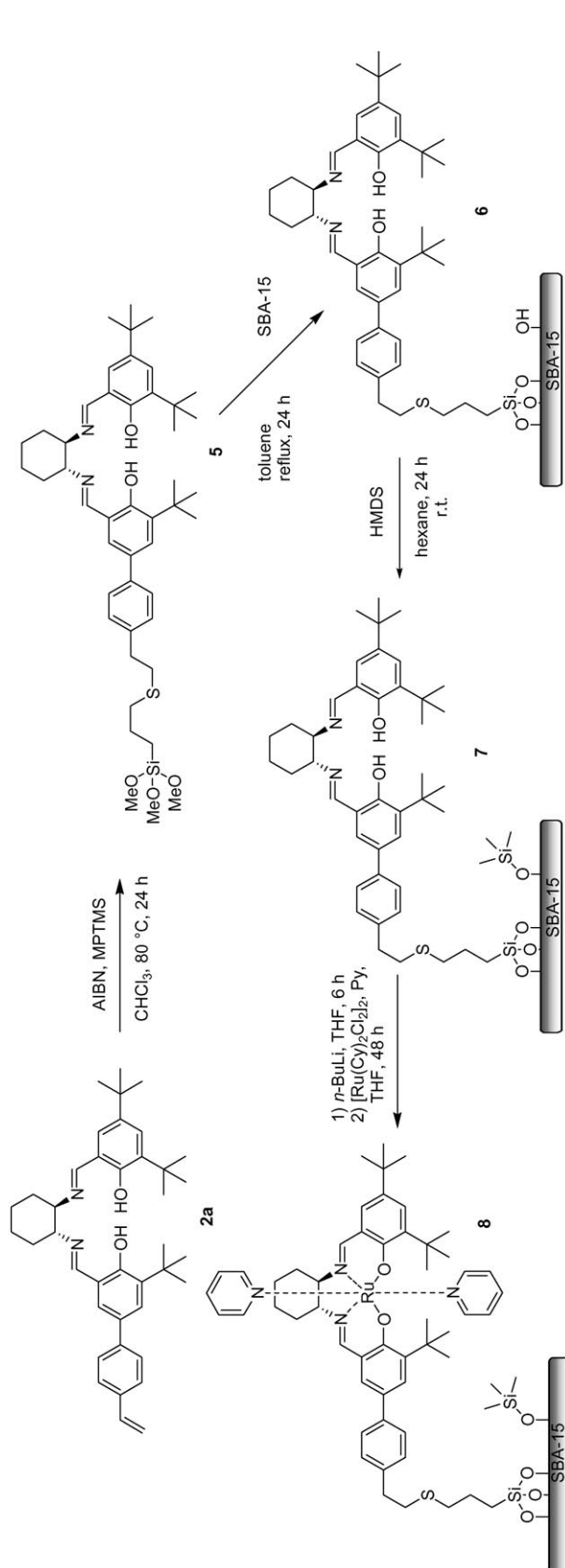


**Figure 1.** FT-IR spectra of (a) non-metallated H<sub>2</sub>salen polymer resin **3b** and (b) metallated Ru(II)-salen-Py<sub>2</sub> polymer resin **4b**.

Upon complexation, this band shifted towards higher frequencies at 1322 cm<sup>-1</sup>. Additionally, the ν<sub>Ru-O</sub> and ν<sub>Ru-N</sub> bands appeared at 539 and 470 cm<sup>-1</sup>, respectively in **4b**.<sup>[24]</sup> These frequency shifts and new bands support coordination of ruthenium to the nitrogen and oxygen of the salen ligand and formation of the Ru(II)-salen-Py<sub>2</sub> complex.

### SBA-15-Supported Ru-Salen Catalyst (**8**): Synthesis and Characterization

Ruthenium-salen bis-pyridine catalyst was also grafted to the surface of SBA-15 mesoporous silica (Scheme 3). A trimethoxysilane-modified, chiral salen



**Scheme 3.** Synthesis of SBA-15-supported Ru(II)-salen bis-pyridine catalyst.

**5** was synthesized *via* thiol coupling of mercaptopropyltrimethoxysilane (MPTMS) with styryl-salen **2a** at 46% isolated yield.<sup>[14,25]</sup> Compound **5** was immobilized on 60 Å mesoporous SBA-15 silica by condensation with surface hydroxy groups forming material **6**. Unreacted silanol groups were capped with hexamethyldisilazane (HMDS) to form material **7** prior to the metallation procedure with *n*-butyllithium and ruthenium dimer. Thermogravimetric analysis (TGA) indicated an organic content of 5.0% and 6.3% for **6** and **7**, respectively. These data equated to a loading of 0.075 mmol salen/g dry silica for **6**. Elemental analysis of **8** indicated a ruthenium loading of 0.031 mmol/g and a N:Ru ratio of 6.2, equating to a 48% metallation efficiency. This moderate metallation efficiency was, again, likely a result of using a stoichiometric amount of *n*-butyllithium and ruthenium dimer in combination with the solid support.

Grafting of salen species on the silica surface was supported by cross-polarization magic-angle spinning (CP MAS)  $^{13}\text{C}$  and  $^{29}\text{Si}$  NMR spectra for material **7** (see Supporting Information). Carbon resonances appeared in the aliphatic region  $\delta = 20\text{--}50$  ppm ( $\text{Si-CH}_2$ ,  $\text{CMe}_3$ ,  $\text{CH}_2$ , cyclohexyl- $\text{CH}_2$ , cyclohexyl- $\text{CH}$ ,  $\text{S-CH}_2$ ,  $\text{Ph-CH}_2$ ), aromatic region  $\delta = 120\text{--}140$  ppm, and imine region  $\delta = 160$  ppm ( $\text{C=N}$ ). In addition to framework silicon  $\text{Q}^2$ ,  $\text{Q}^3$ , and  $\text{Q}^4$  resonances ( $\delta = -94$  to  $-116$  ppm), resonances corresponding to condensation of one to three methoxy groups of compound **5** ( $\delta = -45$  to  $-57$  ppm) appeared in the  $^{29}\text{Si}$  NMR spectrum. The presence of trimethylsilyl capping groups in material **7** was evidenced by the sharp peaks centered at  $\delta = 0.7$  ppm [ $(\text{CH}_3)_3\text{Si}$ ] in the  $^{13}\text{C}$  NMR spectrum and  $\delta = 13$  ppm ( $\text{Me}_3\text{Si-O}$ ) in the  $^{29}\text{Si}$  NMR spectrum.

FT-IR analysis confirmed the presence of organic species in **6–8** by the appearance of aliphatic  $\nu_{\text{C-H}}$  stretch at  $2967\text{ cm}^{-1}$  and imine  $\nu_{\text{C=N}}$  stretch centered at  $1635\text{ cm}^{-1}$  (Figure 2). As expected, the strongest peak in the FT-IR spectra for materials **6–8** corresponded to the  $\nu_{\text{Si-O}}$  stretch from  $1000\text{--}1280\text{ cm}^{-1}$  resulting from the SBA-15 silica support. A strong  $\nu_{\text{O-H}}$  stretch appeared in material **6** from  $3200$  to  $3700\text{ cm}^{-1}$  confirming the presence of surface silanol groups and the inability to react all silanols with bulky compound **5**. This peak diminished but did not disappear in material **7** after the capping step with HMDS possibly due to inaccessible, uncapped silanols and/or the phenolic hydroxy groups in the salen ligand. In conjunction, a sharp peak appeared at  $850\text{ cm}^{-1}$ , corresponding to the  $\nu_{\text{Si-C}}$  stretch in the trimethylsilyl capping groups. Upon metallation with ruthenium, no  $\nu_{\text{O-H}}$  stretch was observed indicating formation of the ruthenium-salen complex.

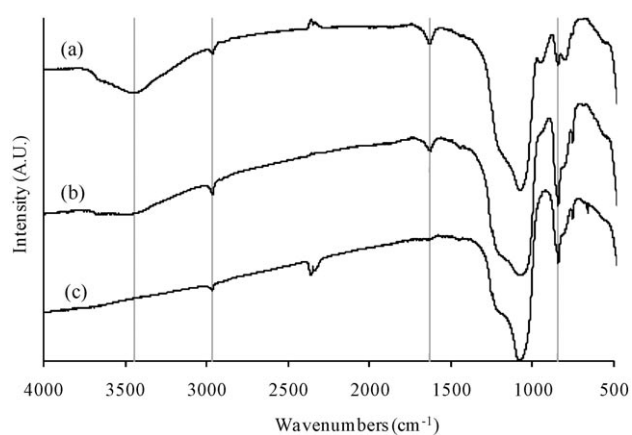


**Figure 2.** FT-IR spectra of (a) SBA-H<sub>2</sub>salen **6**, (b) SBA-H<sub>2</sub>salen capped **7**, and (c) SBA-Ru-salen-Py<sub>2</sub> capped **8**.

### Catalytic Results and Discussion

All cyclopropanation reactions were evaluated in terms of yields, diastereoselectivities (*trans/cis* product ratio), and enantioselectivities (Table 1). Initial reactions using catalysts **4a**, **4b**, and **8** appeared promising (Table 1, entries 2, 5, 8). Yields were similar ( $\geq 95\%$ ), but selectivities of these catalysts suffered slightly in comparison to the homogeneous Ru-salen reported previously.<sup>[3]</sup> Formation of dimeric side products diethyl maleate and diethyl fumarate was not detected *via* GC when using styrene as the olefin reactant. The polymer resin catalysts appeared more active than the silica-based catalyst by reaching  $\geq 95\%$  yield in five hours versus 24 hours. Catalyst **4b** achieved higher selectivities in all areas (10.6 *trans/cis* ratio, 94% *trans*

*ee*, 91% *cis ee*, entry 5) compared to **4a** (8.8 *trans/cis* ratio, 87% *trans ee*, 77% *cis ee*, entry 2), slightly less than that of the homogeneous catalyst (entry 1). Related work using polymer brush-supported Co-salen catalysts for the HKR of epoxides demonstrated a dramatic difference in activity between the rigid styryl and flexible ethylene glycol linkers.<sup>[17]</sup> However, this observation was likely a consequence of the bimetallic mechanism of Co-salen-catalyzed HKR. The Ru-salen-catalyzed cyclopropanation of olefins follows a monometallic mechanism, and therefore, the length/flexibility of the linker should not have as significant an impact on the rates. This seems to be the case, as catalysts **4a** and **4b** appear to be equally active.<sup>[26]</sup>

SBA-15-supported catalyst **8** required longer reaction times to reach high yields than the polymer resin catalysts, but similar selectivities were achieved (9.8 *trans/cis* ratio, 89% *trans ee*, 80% *cis ee*, entry 8). Unfortunately, *ees* were only slightly better than those resulting from catalyst **4a** and less than those of **4b**. The decreased selectivities for **8** may have resulted from steric hindrance with the silica surface. However, a more likely explanation may result from the nature of the silica support itself. In the case of the SBA-15-supported catalyst, it proved impossible to react all silanol groups in bare SBA-15 with excess methoxysilane-modified salen **5** due to the bulky nature of the compound. Consequently, all remaining accessible silanol groups were capped to form material **6** prior to the metallation procedure to prevent reaction with *n*-butyllithium and subsequent immobilization of surface bound, non-chiral, ruthenium species. If any of the silanols present in the mesopores of SBA-15 survived the capping step (or if there are

**Table 1.** Results summary for the cyclopropanation of styrene with various catalysts.<sup>[a]</sup>

Entry	Catalyst	Mol% catalyst	Solvent	Cycle number	Time [h]	Yield [%] <sup>[b]</sup>	<i>trans/cis</i> ratio	<i>trans ee</i> [%] <sup>[c,d]</sup>	<i>cis ee</i> [%] <sup>[d,e]</sup>
1	<b>1</b> <sup>[3]</sup>	1	DCM	1	3	95	10.8	99	96
2	<b>4a</b>	2	DCM	1	4	95	8.8	87	77
3	<b>4a</b>	2	DCM	2	8	80	8.9	88	80
4	<b>4a</b>	2	THF	1	4	91	10.4	84	73
5	<b>4b</b>	2	DCM	1	5	99	10.6	94	91
6	<b>4b</b>	2	DCM	2	8	94	10.9	95	92
7	<b>4b</b>	2	DCM	3	11	93	9.1	95	91
8	<b>8</b>	2	DCM	1	24	95	9.8	89	80
9	<b>8</b>	2	DCM	2	74	49	7.7	80	56
10	<b>8</b>	2	THF	1	24	79	12.1	79	67
11	<b>8</b>	2	THF	2	24	17	10.0	77	62

<sup>[a]</sup> Initial reactions performed using 0.5 mmol EDA, 2.5 mmol styrene, 3.5 mL solvent, and 0.5 mmol tridecane (internal standard) at room temperature inside a glove box.

<sup>[b]</sup> Determined *via* GC calibration.

<sup>[c]</sup> Enantioselectivity towards the (1*R*,2*R*) product.

<sup>[d]</sup> Determined *via* chiral GC.

<sup>[e]</sup> Enantioselectivity towards the (1*R*,2*S*) product.

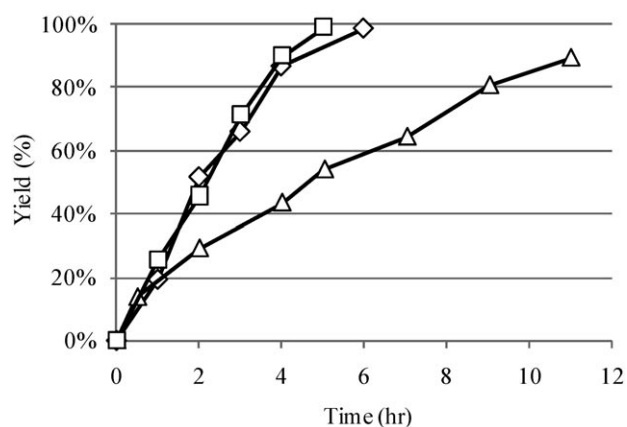


**Figure 3.** Yield of cyclopropyl products versus time using catalyst **4b**: (□) first cycle, (△) third cycle, and (◇) third cycle with pyridine treatment between all previous cycles.

many oxygens associated with siloxane bridges accessible to the metal center), then they could create adverse interactions with the Ru-salen catalyst, potentially explaining the decreased *ees*, as seen experimentally.

It should be noted that extensive studies were performed trying to replicate previous metallation procedures<sup>[27]</sup> that used triethylamine instead of a stronger deprotonating agents such lithium diisopropylamide used previously<sup>[3]</sup> or *n*-butyllithium in this work. However, the proposed Ru-salen could never be isolated using homogeneous or heterogeneous salens under a variety of conditions. For example, when metallating the supported salens in this way, filtration with DCM always removed the brownish/red color associated with the ruthenium, resulting in no color change to the parent material. In both cases, no active cyclopropanation catalyst was ever isolated. For this reason, the stronger deprotonating agent was used.

Recycle studies using catalysts **4a**, **4b**, and **8** displayed very similar diastereoselectivities and enantioselectivities as the initial runs, but decreased rates were observed, leading to longer reaction times (Table 1, entries 3, 6, 7, 9). Catalyst **4b** required over twice as long to reach 95% yield in the third run (11 h) versus the first run (5 h) (Figure 3). These data may suggest a fractional loss of active Ru-salen species with each successive cycle, possibly due to leaching of ruthenium during the washing steps between cycles or catalyst poisoning. Studies using THF as a solvent instead of DCM resulted in lower yields and *ees* but curiously higher diastereoselectivities (entries 4 and 10). Recycle studies using THF solvent displayed similar losses in catalytic activity as using DCM (entry 11).

To fully understand the catalytic activities, kinetic data were collected rather than analyzing single point

yields at long times, as is commonly done in the literature. Reporting single point yields at long times can be misleading, as this practice can mask the true kinetics, activity, recyclability, and deactivation. The yields reported in this paper are not collected at long times. Instead kinetics were collected for most reactions and yields are reported at the corresponding times. Figure 3 displays representative data for the deactivation of polymer resin catalyst **4b**. An analogous figure for catalyst **4a** appears in the Supporting Information. Using kinetic data, instead of single point yields, a clearer picture of catalyst deactivation can be observed between the first and third cycle for catalyst **4b**.

Catalyst deactivation proved to be an initial hurdle during this work. However, it was observed this could be minimized by the addition of pyridine during the washing steps between cycles. Addition of pyridine to each washing step proved to have a positive effect on catalyst stability over several cycles as seen by overlapping kinetics between the first cycle and third cycle with pyridine treatment (Figure 3). As a result, all recycle experiments were repeated using the pyridine treatment between cycles (Table 2). At slightly longer times (6 h), very high yields ( $\geq 97\%$ ) could be achieved for both polymer resin catalysts over the three cycles tested without any apparent deactivation (Table 2, entries 1–6). Initial cycles gave similar results as shown in Table 1, and subsequent cycles showed marginally better selectivities (entries 1–2, 4–5). This marginal increase may result from removal of any residual, non-chiral ruthenium species that may not have been removed during the filtration steps following the metallation procedure. Catalysts **4a** and **4b** displayed very consistent yields and selectivities over three cycles, with catalyst **4b** approaching the performance of the homogeneous Ru-salen except for overall activity (entry 5).

The addition of excess pyridine during the washing steps is thought to stabilize the ruthenium center during the washing procedure. The Ru(II)-salen bis-pyridine complex must dissociate a pyridine ligand prior to entering the catalytic cycle. This vacant coordination site permits formation of the ruthenium carbene intermediate prior to carbene addition across the carbon-carbon double bond of the olefin. After complete consumption of the EDA and ruthenium carbene by excess styrene, a vacant coordination site remains on the ruthenium center. Addition of excess pyridine shifts the equilibrium towards binding two pyridine ligands, thus stabilizing the Ru-salen complex, and inhibiting leaching of ruthenium metal from the ligand. Elemental analysis data indicated that pyridine washing did affect the ruthenium content in the recycled catalysts. Compared to the fresh catalyst **4a**, the used catalyst after three cycles using the pyridine treatment retained 85% of the initial ruthenium con-

**Table 2.** Results summary for the cyclopropanation of styrene with various catalysts by modified recycling method.<sup>[a]</sup>

Entry	Catalyst	Mol% catalyst	Solvent	Cycle number	Time [h]	Yield [%] <sup>[b]</sup>	<i>trans/cis</i> ratio	<i>trans ee</i> [%] <sup>[c,d]</sup>	<i>cis ee</i> [%] <sup>[d,e]</sup>
1	<b>4a</b>	2	DCM	1	6	97	9.1	90	82
2	<b>4a</b>	2	DCM	2	6	97	9.4	93	88
3	<b>4a</b>	2	DCM	3	6	99	8.9	91	86
4	<b>4b</b>	2	DCM	1	6	97	10.7	94	90
5	<b>4b</b>	2	DCM	2	6	99	10.9	96	95
6	<b>4b</b>	2	DCM	3	6	99	10.6	96	93
7	<b>8</b>	1	DCM	1	24	27	7.5	81	56
8	<b>8</b>	1	DCM	2	24	20	7.7	85	50
9	<b>8</b>	1	DCM	3	48	15	6.3	80	35
10	<b>8</b>	1	THF	1	24	18	8.0	73	42
11	<b>8</b>	1	THF	2	24	15	7.0	75	45
12	<b>8</b>	1	THF	3	48	11	5.2	69	32

<sup>[a]</sup> Initial reactions performed using 0.5 mmol EDA, 2.5 mmol styrene, 3.5 mL solvent, and 0.5 mmol tridecane (internal standard) at room temperature inside a glove box.

<sup>[b]</sup> Determined *via* GC calibration.

<sup>[c]</sup> Enantioselectivity towards the (1*R*,2*R*) product.

<sup>[d]</sup> Determined *via* chiral GC.

<sup>[e]</sup> Enantioselectivity towards the (1*R*,2*S*) product.

**Table 3.** Elemental analysis comparison between fresh and recycled catalyst **4a**.

Catalyst	% Ru	% N	Ru loading [mmol g] <sup>-1</sup>	Relative Ru content	N/Ru mol ratio
Fresh	3.4%	2.9%	0.34	100%	6.2
3rd Cycle (with Py)	2.9%	2.8%	0.29	85%	7.0
3rd Cycle (No Py)	2.5%	2.7%	0.24	72%	7.8

ment (Table 3). Without the addition of pyridine, the ruthenium content dropped to 72% of the fresh catalyst. Furthermore, the nitrogen to ruthenium mol ratio increased from an initial value of 6.2 (indicating an incomplete metallation procedure, since an Ru-salen-Py<sub>2</sub> complex should have N/Ru=4) for the fresh catalyst to 7.0 and 7.8 for the recycled catalysts with and without the pyridine treatments, respectively.

Attempts to assess changes to the Ru-salen catalysts upon recycling *via* FT-IR analysis proved inconclusive owing to overlapping peaks from pyridine (1633 and 1598 cm<sup>-1</sup>) and the imine peaks of interest (1631 and 1607 cm<sup>-1</sup>, see Supporting Information).<sup>[13]</sup> No apparent differences between the fresh and spent catalysts were observed in the ν<sub>C-O</sub> stretching region (commonly 1275 cm<sup>-1</sup> for non-metallated and 1310 cm<sup>-1</sup> for the metallated ruthenium Schiff base complexes).<sup>[22–24,28]</sup> In addition, the ν<sub>Ru-N</sub> and ν<sub>Ru-O</sub> stretches (450 cm<sup>-1</sup> and 530 cm<sup>-1</sup>, respectively) were only minutely visible, due to the low ruthenium loadings on the solid supports compared to analogous studies of homogeneous small molecule complexes.

Catalyst **8** showed less consistent results over three cycles and its selectivities were moderate in compari-

son to the polymer resin-supported catalysts, indicating such a sensitive catalyst may be more difficult to immobilize on silicas or other inorganic oxides, where potentially deleterious interactions with surface hydroxy groups or siloxane bridges may be present. This result appears in agreement with siliceous mesocellular foam (MCF)-supported Cu-Box and Cu-PyBox investigations in which the authors suggest capping of surface hydroxy groups was paramount to the activity and stability of the cyclopropanation catalyst.<sup>[29]</sup> More detailed studies of the silica-supported Ru-salen system are needed.

The Ru-salen polymer resin catalysts (**4a**, **4b**) compare extremely favorably against the best supported copper bis(oxazoline) catalysts to date.<sup>[6]</sup> While the supported Ru-salen and Cu-Box catalysts exhibit comparable activities and enantioselectivities (generally >90%), Ru-salen catalysts exhibit extremely high yields and are about four times more diastereoselective to the *trans* products (*trans/cis*=9–11) than the Cu-Box systems (generally *trans/cis*=2–3).<sup>[30]</sup> Additionally, use of Ru-salen catalysts requires no activation step, unlike the Cu-Box systems, which require addition of phenylhydrazine prior to reaction. Supported Ru-salen catalysts also supercede Ru-porphyr-

**Table 4.** Summary of results for the cyclopropanation of various terminal olefins with catalyst **4b**.<sup>[a]</sup>

Entry	Olefin	Solvent	Time [h]	Conversion [%]	Yield [%] <sup>[b]</sup>	<i>trans/cis</i> ratio	<i>trans ee</i> [%] <sup>[c,d]</sup>	<i>cis ee</i> [%] <sup>[d,e]</sup>
1	Pentene	DCM	39	93	5.0	2.7	54	34
2	EVE	Neat	24	75	7.5	2.1	36	33
3	EVE	DCM	48	85	13	2.3	50	80
4	MMA	DCM	52	100	36	10.1	−7.5	−26
5	Piperylene	DCM	48	100	48	1.6	55	55
6	Styrene	DCM	6	100	97	10.7	94	90

<sup>[a]</sup> Reactions performed using 0.25 mmol EDA, 1.25 mmol olefin, 1.75 mL solvent, and 0.25 mmol tridecane (internal standard) at room temperature inside a glove box.

<sup>[b]</sup> Determined *via* GC calibration.

<sup>[c]</sup> Enantioselectivity towards the (1*R*,2*R*) product.

<sup>[d]</sup> Determined *via* chiral GC.

<sup>[e]</sup> Enantioselectivity towards the (1*R*,2*S*) product.

rin<sup>[11]</sup> and Ru-PyBox<sup>[7]</sup> catalysts in terms of yields and enantioselectivities, but are comparable in diastereoselectivity.

After successful cyclopropanation studies using styrene, the utility of supported Ru-salen catalysts on a range of electronically diverse terminal olefins was investigated. These studies examined the most active and selective catalyst **4b** at 2 mol% catalyst (Table 4). Generally, the more activated olefins resulted in higher yields of cyclopropanated products. The differences between the product yields and ethyl diazoacetate (EDA) conversions resulted from formation of dimeric side products diethyl maleate and diethyl fumarate and minor amounts of trimer side product, presumably triethyl cyclopropane-1,2,3-tricarboxylate. Cyclopropanation of pentene resulted in very low yields (5%) of product at moderate enantioselectivity. Improved yields and selectivities of products were observed using ethyl vinyl ether (EVE). In contrast to studies using the homogeneous catalyst, the use of solvent instead of neat olefin resulted in significant improvements to the *ees* and moderate increases in yield and diastereoselectivity. This difference likely resulted from positive solvent swelling effects of DCM on the polymer resin, reducing steric hindrance near the active site. The homogeneous Ru-salen catalyst would not experience these issues, explaining why no difference was observed between neat and solvated reactions.<sup>[3]</sup> As a result of this observation, all studies using different olefins were performed using solvent. Contrary to the case with homogeneous Ru-salen where very minimal *cis* products were observed (100 *trans/cis* ratio),<sup>[3]</sup> appreciable amounts of *cis* products from the cyclopropanation of methyl methacrylate (MMA) were observed using catalyst **4b** (10.1 *trans/cis* ratio). Consistently, a reversal in enantioselectivity of the MMA cyclopropanation products was observed using chiral GC, showing 7.5% *trans ee* (1*S*,2*S*) and 26% *cis ee* (1*S*,2*R*). Cyclopropanation of *trans* piperylene generated the highest product yields

of the olefins studied, with moderate enantioselectivities and low diastereoselectivity (Table 4, entry 5).

## Conclusions

This work demonstrates the first report of covalently grafted Ru-salen complexes on solid supports. These catalysts were observed to be highly active, selective, and recyclable for use in the asymmetric cyclopropanation of olefins useful in the pharmaceutical and agro-chemical industries. Two polymer resin- and one SBA-15-supported Ru(II)-salen bis-pyridine catalyst were synthesized and tested in the cyclopropanation of styrene. All three generated the desired products in high yield and *trans* selectivity with moderate to high enantioselectivities. Polymer resin catalyst **4b** was observed to generate products with the highest selectivities and yield, an observation potentially occurring from lessened steric hindrance due to the lengthened linker between the Ru-salen active site and polymer support. Fractional losses in activity were observed upon recycle of these catalysts while product selectivities were unchanged. However, addition of pyridine during the washing steps between cycles was observed to retain the high activities of the polymer resin catalysts after three cycles by stabilizing the complex between cycles and decreasing leaching of ruthenium. Moderate enantioselectivities were observed using the SBA-15-supported catalyst **8**, possibly due to adverse reactions with the silica surface. Additional studies with other terminal olefins demonstrated better catalyst performance for the more activated olefins, consistent with previous reports. In contrast to the homogeneous case, the use of solvent resulted in increased yields and selectivities, presumably by making the active site more accessible and less hindered inside the swollen polymer resin. These solid-supported analogues of homogeneous Ru-salen catalysts show promise in the facile recycling of these

expensive catalysts for repeated processes. Additionally, polymer resin-supported Ru-salen catalysts **4a** and **4b** generated superior selectivities and yields versus other leading solid-supported, asymmetric cyclopropanation catalysts.

## Experimental Section

### General Remarks

All chemicals were purified prior to use and stored in a nitrogen glove box, and all reactions were initiated in the glove box. Dichloromethane (DCM) was distilled over calcium hydride. Tetrahydrofuran (THF) and toluene were distilled over sodium. Hexane (<50 ppm water) was further dried over columns of activated copper oxide and alumina.<sup>[31]</sup> Styrene was washed to remove inhibitors (5% NaOH, water, and brine), dried over magnesium sulfate, distilled over calcium hydride, and stored at  $-23^{\circ}\text{C}$  in the glove box prior to use. Divinylbenzene was washed to remove inhibitors (5% NaOH, water, and brine) and dried over sodium sulfate immediately prior to use. Tridecane was dried over calcium hydride, vacuum distilled, and stored in the glove box. Ethyl diazoacetate (EDA) was degassed *via* three freeze-pump-thaw cycles and stored in the glove box at  $-23^{\circ}\text{C}$ .

### Instrumentation

Cross-polarization magic angle spinning (CP-MAS) solid-state NMR spectra were measured using a Bruker DSX 300 MHz spectrometer. Samples were packed in 7 mm zirconia rotors and spun at 6.6 kHz. Solid state  $^{13}\text{C}$  CP-MAS spectra were recorded using 3000 scans, a  $90^{\circ}$  pulse length of 4  $\mu\text{s}$ , and recycle times of 4 s. Solid state  $^{29}\text{Si}$  CP-MAS were recorded using 5000 scans, a  $90^{\circ}$  pulse length of 5  $\mu\text{s}$ , and recycle times of 5 s. Conversions of ethyl diazoacetate (EDA), product yields (*via* calibration curves from pure samples), and *trans/cis* product ratios were calculated using capillary gas-phase chromatography on a Shimadzu GC 2010 equipped with an FID detector and a SHRX5 column (15 m  $\times$  0.25 mm  $\times$  0.25  $\mu\text{m}$ ). The oven profile heated from  $50^{\circ}\text{C}$  to  $250^{\circ}\text{C}$  at  $10^{\circ}\text{C}/\text{min}$ . When using styrene as the olefin, enantiomeric excesses of the *trans* cyclopropyl products were measured on a Shimadzu GC 2010 equipped with an FID detector and a Beta DEX 225 column (30 m  $\times$  0.25 mm  $\times$  0.25  $\mu\text{m}$ ). The oven profile heated from  $100^{\circ}\text{C}$  to  $140^{\circ}\text{C}$  at  $0.5^{\circ}\text{C}/\text{min}$ . *cis*-Cyclopropyl products were measured on a Shimadzu 14 A GC with an FID detector and an Astec ChiralDEX  $\gamma$ -TA column (40 m  $\times$  0.25 mm  $\times$  0.12  $\mu\text{m}$ ) using the same oven profile as the *trans* products. When using other olefins, similar analytical methods were used as previously reported.<sup>[3]</sup> A Netzsch Thermoanalyzer STA 409 was used for thermogravimetric analysis (TGA) and differential scanning calorimetry (DSC) with a heating rate of  $10^{\circ}\text{C}/\text{min}$  in air. Elemental analyses were performed by Columbia Analytics Lab (Tucson, AZ, USA) or Galbraith Laboratories, Inc. (Knoxville, TN, USA).

### Synthesis of Insoluble Polymer Resin-Supported Ru(II)-Salen Bis-pyridine Catalysts (**4a**) and (**4b**)

An insoluble polymer resin was synthesized by combining divinylbenzene (521 mg, 4 mmol, inhibitors removed and freshly dried), styryl-salen<sup>[15,17,19]</sup> (593 mg for **4a**, 681 mg for **4b**, 1 mmol), and AIBN (44 mg, 0.27 mmol) in chlorobenzene (2.2 g). The reaction mixture was stirred under argon ( $80^{\circ}\text{C}$ , 48 h). The solid polymer resin was recovered *via* filtration and washed with copious methanol, hexane, DCM, THF, and ether. The resin was ground to a powder with a mortar and pestle, filtered again, and dried under high vacuum (room temperature, 12 h). The salen polymer resin was then metallated with ruthenium using a slightly modified procedure from the literature.<sup>[3]</sup> Inside a glove box, *n*-butyllithium (1.6 M in hexane, 170 mg, 0.4 mmol) was added to a mixture of polymer resin (containing 0.2 mmol of salen) and THF (1.44 g) cooled to  $-23^{\circ}\text{C}$ . The mixture was stirred and allowed to warm to room temperature (6 h). A mixture of  $[\text{Ru}(\text{Cy})_2\text{Cl}_2]_2$  (61 mg, 0.1 mmol), THF (2.1 g), and pyridine (127 mg, 1.6 mmol) was added to the lithiated polymer mixture and stirred at room temperature inside the glove box (48 h). The metallated Ru-salen polymer resin was recovered *via* filtration and washed with copious THF, methanol, DCM, toluene, hexane, and ether. The resulting dark brown solid was dried under high vacuum at room temperature overnight and stored in the glove box.

### Synthesis of SBA-15-Supported Ru(II)-Salen Bis-pyridine Catalyst (**8**)

SBA-15 was synthesized according to published procedures,<sup>[32]</sup> dried under high vacuum ( $250^{\circ}\text{C}$ , 3 h), and stored in a nitrogen glove box. A silane-modified salen species **5** was synthesized using procedures developed within our research group.<sup>[14]</sup> The salen was post-grafted to the SBA-15 support by refluxing silane-modified salen **5** (290 mg) and SBA-15 (1.7 g) in anhydrous toluene (16 g) under argon (24 h). The resulting solid was recovered *via* filtration and washed with copious toluene, DCM, hexane, and ether. The salen-functionalized SBA-15 **6** was dried under high vacuum at room temperature (12 h). Unreacted SBA surface hydroxy groups were then capped by stirring salen-functionalized SBA-15 **6** (500 mg) and hexamethyldisilazane (HMDS, 500 mg) in hexane (10 g) under argon at room temperature (48 h). The capped salen-modified SBA-15 **7** was recovered *via* filtration, washed with hexane, toluene, DCM, hexane, and ether, and dried overnight at room temperature under high vacuum. The capped, salen-functionalized SBA-15 was then metallated with ruthenium similar to the procedure described above. Inside a glove box, *n*-butyllithium (1.6 M in hexane, 54 mg, 0.13 mmol) was added to a mixture of capped, salen-modified SBA-15 **7** (494 mg, 0.064 mmol salen ligand) and THF (460 mg) cooled to  $-23^{\circ}\text{C}$ . The mixture was stirred and allowed to warm to room temperature (6 h). A mixture of  $[\text{Ru}(\text{Cy})_2\text{Cl}_2]_2$  (20 mg, 0.032 mmol), THF (690 mg), and pyridine (40 mg, 0.51 mmol) was added to the lithiated SBA-15 mixture and stirred at room temperature inside the glove box (48 h). The metallated Ru-salen SBA-15 **8** was recovered *via* filtration and washed with copious

THF, methanol, DCM, toluene, hexane, and ether. The resulting dark brown solid was dried under high vacuum at room temperature overnight and stored in the glove box.

### General Procedure for Cyclopropanation Reactions

All cyclopropanation reactions were carried out inside a nitrogen glove box. Prior to reaction, the mass of the empty flask and stir bar was recorded. Ru-salen catalyst (0.01 mmol, 0.02 equiv.), DCM (1 mL), and styrene (260 mg, 2.5 mmol, 5 equiv.) were added to the 10-mL pear-shaped flask. A solution of DCM (2.5 mL), tridecane (92.2 mg, 1 equiv.), and EDA (65 mg, 1 equiv., 88 wt% in DCM by  $^1\text{H}$  NMR) was added dropwise over a 20-min period to the catalyst solution to initiate the reaction. Samples (20  $\mu\text{L}$ ) were periodically removed and filtered with acetone (1 mL) through silica gel and a cotton plug to remove the catalyst. The samples were analyzed *via* GC with reference to the tridecane internal standard. Upon completion, the reaction mixture was diluted with THF (3 mL). The catalyst was allowed to settle gravimetrically and the solution was removed *via* pipette. This procedure was repeated once with THF and twice more with ethyl ether. For the recycling experiments using the pyridine treatment, pyridine (10  $\mu\text{L}\cdot\text{mg}^{-1}$  catalyst, generally 300  $\mu\text{L}$ ) was added to each wash cycle. The catalyst was dried under vacuum and returned to the glove box. All recycle experiments were scaled to the mass of recovered catalyst due to losses during each cycle from sampling and washing (typically 13% loss per cycle).

### Acknowledgements

The authors acknowledge financial support of this work by the DOE-BES through Catalysis Science contract DE-FG02-03ER15459. We also thank Dr. Carsten Sievers for assistance obtaining solid state NMR spectra.

### References

- [1] a) W. A. Donaldson, *Tetrahedron* **2001**, *57*, 8589; b) J. Salaun, *Chem. Rev.* **1989**, *89*, 1247; c) O. Lopez, J. G. Fernandez-Bolanos, M. V. Gil, *Green Chem.* **2005**, *7*, 431.
- [2] a) M. P. Doyle, D. C. Forbes, *Chem. Rev.* **1998**, *98*, 911; b) M. P. Doyle, M. N. Protopopova, *Tetrahedron* **1998**, *54*, 7919; c) H. Lebel, J. F. Marcoux, C. Molinaro, A. B. Charette, *Chem. Rev.* **2003**, *103*, 977; d) H. Pellissier, *Tetrahedron* **2008**, *64*, 7041; e) G. Maas, *Chem. Soc. Rev.* **2004**, *33*, 183; f) T. Katsuki, *Adv. Synth. Catal.* **2002**, *344*, 131; g) T. Katsuki, *Synlett* **2003**, 281.
- [3] J. A. Miller, W. C. Jin, S. T. Nguyen, *Angew. Chem.* **2002**, *114*, 3077; *Angew. Chem. Int. Ed.* **2002**, *41*, 2953.
- [4] a) J. A. Miller, E. J. Hennessy, W. J. Marshall, M. A. Scialdone, S. T. Nguyen, *J. Org. Chem.* **2003**, *68*, 7884; b) J. A. Miller, B. A. Gross, M. A. Zhuravel, W. C. Jin, S. T. Nguyen, *Angew. Chem.* **2005**, *117*, 3953; *Angew. Chem. Int. Ed.* **2005**, *44*, 3885.
- [5] a) C. E. Song, S. G. Lee, *Chem. Rev.* **2002**, *102*, 3495; b) S. Bräse, F. Lauterwasser, R. E. Ziegert, *Adv. Synth. Catal.* **2003**, *345*, 869.
- [6] J. M. Fraile, J. I. Garcia, J. A. Mayoral, *Coord. Chem. Rev.* **2008**, *252*, 624.
- [7] A. Cornejo, J. M. Fraile, J. I. Garcia, M. J. Gil, S. V. Luis, V. Martinez-Merino, J. A. Mayoral, *J. Org. Chem.* **2005**, *70*, 5536.
- [8] A. Cornejo, J. M. Fraile, J. I. Garcia, E. Garcia-Verdugo, M. J. Gil, G. Legarreta, S. V. Luis, V. Martinez-Merino, J. A. Mayoral, *Org. Lett.* **2002**, *4*, 3927.
- [9] A. Cornejo, J. M. Fraile, J. I. Garcia, M. J. Gil, V. Martinez-Merino, J. A. Mayoral, *Tetrahedron* **2005**, *61*, 12107.
- [10] A. Cornejo, J. M. Fraile, J. I. Garcia, M. J. Gil, S. V. Luis, V. Martinez-Merino, J. A. Mayoral, *C. R. Chim.* **2004**, *7*, 161.
- [11] Y. Ferrand, P. Le Maux, G. Simonneaux, *Tetrahedron: Asymmetry* **2005**, *16*, 3829.
- [12] J. L. Zhang, Y. L. Liu, C. M. Che, *Chem. Commun.* **2002**, 2906.
- [13] S. Syukri, W. Sun, F. E. Kühn, *Tetrahedron Lett.* **2007**, *48*, 1613.
- [14] C. S. Gill, K. Venkatasubbaiah, N. T. S. Phan, M. Weck, C. W. Jones, *Chem. Eur. J.* **2008**, *14*, 7306.
- [15] a) M. Holbach, M. Weck, *J. Org. Chem.* **2006**, *71*, 1825; b) X. L. Zheng, C. W. Jones, M. Weck, *Chem. Eur. J.* **2006**, *12*, 576.
- [16] X. L. Zheng, C. W. Jones, M. Weck, *J. Am. Chem. Soc.* **2007**, *129*, 1105.
- [17] X. L. Zheng, C. W. Jones, M. Weck, *Adv. Synth. Catal.* **2008**, *350*, 255.
- [18] S. Jain, X. L. Zheng, C. W. Jones, M. Weck, R. J. Davis, *Inorg. Chem.* **2007**, *46*, 8887.
- [19] M. Holbach, X. L. Zheng, C. Burd, C. W. Jones, M. Weck, *J. Org. Chem.* **2006**, *71*, 2903.
- [20] A. Heckel, D. Seebach, *Helv. Chim. Acta* **2002**, *85*, 913.
- [21] N. Madhavan, C. W. Jones, M. Weck, *Acc. Chem. Res.* **2008**, *41*, 1153.
- [22] S. Kannan, R. Ramesh, *Polyhedron* **2006**, *25*, 3095.
- [23] K. N. Kumar, G. Venkatachalam, R. Ramesh, Y. Liu, *Polyhedron* **2008**, *27*, 157.
- [24] M. S. Refat, S. A. Ei-Korashy, D. N. Kumar, A. S. Ahmed, *Spectrochim. Acta Part A* **2008**, *70*, 898.
- [25] C. Baleizao, B. Gigante, H. Garcia, A. Corma, *J. Catal.* **2003**, *215*, 199.
- [26] The slight difference in selectivities between **4a** and **4b** may possibly be explained by the shorter linker of **4a** compared to **4b**. Due to the closer proximity of the polymer backbone to the Ru-salen active site for **4a**, increased steric interference may be causing the slight drop in selectivity. The longer, flexible linker of **4b** may lessen the steric hindrance, thereby producing higher selectivities.
- [27] J. L. Liang, X. Q. Yu, C. M. Che, *Chem. Commun.* **2002**, 124.
- [28] L. Mishra, R. Prajapati, K. K. Pandey, *Spectrochim. Acta Part A* **2008**, *70*, 79.
- [29] S. S. Lee, S. Hadinoto, J. Y. Ying, *Adv. Synth. Catal.* **2006**, *348*, 1248; a) S. S. Lee, J. Y. Ying, *J. Mol. Catal. A: Chem.* **2006**, *256*, 219.

- [30] a) J. M. Fraile, J. I. Garcia, C. I. Herrerias, J. A. Mayoral, S. Gmough, M. Vaultier, *Green Chem.* **2004**, *6*, 93; b) J. H. Lim, S. N. Riduan, S. S. Lee, J. Y. Ying, *Adv. Synth. Catal.* **2008**, *350*, 1295; c) A. Mandoli, S. Orlandi, D. Pini, P. Salvadori, *Chem. Commun.* **2003**, 2466; d) H. Werner, C. I. Herrerias, M. Glos, A. Gissibl, J. M. Fraile, I. Perez, J. A. Mayoral, O. Reiser, *Adv. Synth. Catal.* **2006**, *348*, 125.
- [31] A. B. Pangborn, M. A. Giardello, R. H. Grubbs, R. K. Rosen, F. J. Timmers, *Organometallics* **1996**, *15*, 1518.
- [32] a) D. Y. Zhao, Q. S. Huo, J. L. Feng, B. F. Chmelka, G. D. Stucky, *J. Am. Chem. Soc.* **1998**, *120*, 6024; b) J. C. Hicks, C. W. Jones, *Langmuir* **2006**, *22*, 2676.
-